International Journal of Solids and Structures 49 (2012) 2418–2423

Contents lists available at SciVerse ScienceDirect

International Journal of Solids and Structures

journal homepage: www.elsevier.com/locate/ijsolstr

Cooperative deformation of carboxyl groups in functionalized carbon nanotubes

Arun K. Nair [a,b], Zhao Qin [a,b], Markus J. Buehler [a,b,c,*]

[a] Laboratory for Atomistic and Molecular Mechanics (LAMM), Department of Civil and Environmental Engineering, Massachusetts Institute of Technology, 77 Massachusetts Ave., Room 1-235A, USA
[b] Center for Computational Engineering, Massachusetts Institute of Technology, 77 Massachusetts Ave., Cambridge, MA 02139, USA
[c] Center for Materials Science and Engineering, Massachusetts Institute of Technology, 77 Massachusetts Ave., Cambridge, MA 02139, USA

ARTICLE INFO

Article history:
Received 12 February 2012
Received in revised form 7 April 2012
Available online 23 May 2012

Keywords:
Bio-inspired
Fiber
Mechanical properties
Deformation
Cooperativity
H-bonds
Functionalization
Carbon nanotubes

ABSTRACT

Functionalized carbon nanotubes have tremendous potential for nanotechnology applications such as in the fabrication of polymeric carbon fibers. However, approaches to design carbon nanotube structures by using functional groups as glue and carbon nanotubes as stiff building blocks to reach superior mechanical strength and toughness at the fiber level with limited amount of materials remains poorly understood. Inspired by the outstanding mechanical properties of spider silk, here we present a bio-inspired structural model of carbon nanotube based fibers connected by weak hydrogen bonds (H-bonds) formed between functional carboxyl groups as the molecular interface. By applying shear loading, we study how the deformation of H-bonds in functional groups is affected by the structural organization of the carboxyl groups, as well as by the geometry of constituting carbon nanotubes. The analysis of H-bond deformation fields is used to compute the extent of significant deformation of inter-CNT bonds, defining a region of cooperativity. We utilize an exponential function ($\exp(-x/\xi)$) to fit the deformation of H-bonds, with the cooperative region defined by the parameter ξ, and where a higher value of ξ represents a weaker exponential decay of displacements of carboxyl groups from the point where the load is applied. Hence, the parameter ξ characterizes the number of carboxyl groups that participate in the deformation of CNTs under shear loading. The cooperativity of deformation is used as a measure for the utilization of the chemical bonds facilitated by the functional groups. We find that for ultra-small diameter CNTs below 1 nm the external force deforms H-bonds significantly only within a relatively small region on the order of a few nanometers. We find that the mechanical properties of carbon nanotube fibers are affected by the organization of H-bonds in functional carboxyl groups. Both, the grouping of functional groups into clusters, and a specific variation of the clustering of functional groups along the CNT axis are shown to be potential strategies to improve the cooperativity of deformation. This allows for a more effective utilization of functional groups and hence, larger overlap lengths between CNTs in fibers. The effect of structural organization of functional groups is not only significant in very small diameter CNTs, but also in larger diameter CNTs as they are most commonly used for engineering applications. Notably larger-diameter CNTs naturally show a larger cooperative deformation range. Our model can be applied to other functional groups attached to CNTs, and could in principle also include strong bonds such as covalent or ionic bonds, or other weak bonds such van der Waals forces or dipole–dipole interactions.

1. Introduction

Carbon nanotubes (CNTs) (Iijima, 1991) have been studied extensively for the past two decades. The excellent physical and chemical properties of CNTs have made them a prime candidate for applications in various technologies. Moreover, functionalized carbon nanotubes have received much attention in the past decade due to their wide range of applications spanning several fields including structural materials, fibers and yarns, electronic devices, and biology. Specific applications include sensors, drug design and discovery, photovoltaic devices and reinforcement for polymer nanocomposites, or even conceptional designs for a space elevator (Fam et al., 2011; Su et al., 2011; Kong et al., 2001; Dhullipudi et al., 2005; Prato et al., 2006; Pugno 2006; Koziol et al., 2007; Ostojic et al., 2008; Kostarelos et al., 2009; Bratzel et al., 2010; Guo et al., 2010; Tang et al., 2011). Specifically, the use of functionalized multiwall CNTs in nanocomposites have shown to improve their mechanical and thermal properties by forming stronger chemical bonds across interfaces, and opened exciting opportunities for

* Corresponding author at: Center for Materials Science and Engineering, Massachusetts Institute of Technology, 77 Massachusetts Ave., Cambridge, MA 02139, USA. Tel.: +1 617 452 2750; fax: +1 617 324 4014.
E-mail address: mbuehler@MIT.EDU (M.J. Buehler).

0020-7683/$ - see front matter © 2012 Elsevier Ltd. All rights reserved.
http://dx.doi.org/10.1016/j.ijsolstr.2012.05.002

high-impact applications (Amr et al., 2011; Choudhury and Kar, 2011; Coleman et al., 2006; Ganguli et al., 2008; Cheng et al., 2010; Zhu et al., 2010; Cornwell and Welch, 2011).

However, a crucial issue for structural applications of CNT based materials is that individual CNTs cannot be grown to relevant scales of meters and beyond. This necessitates a need to connect distinct CNTs such that mechanical strong interfaces are created. Functionalized CNTs can be used to extend the effective CNT length, to create longer fibers that reach macroscale dimensions, by connecting them through chemical groups, which serve as a chemical glue, attached to their surface. Functional groups can be, for example, carboxyl (COOH) groups as shown in Fig. 1(a). Here, each carboxyl group has an oxygen atom, which is covalently bonded to the hydrogen atom and acts as a donor. Another oxygen atom acts as an acceptor for the hydrogen bond. Therefore, two hydrogen bonds (H-bonds) form between two pairing carboxyl groups. A variety of other functional groups (e.g. OH, NH_n, CH_n) can be explored to engineer the bonding between functionalized CNTs (Chen et al., 2002; Peng et al., 2008; Jacobs et al., 2011). Despite these superior properties that can potentially be exhibited by multiwall functionalized nanotubes, few studies have been conducted to systematically understand and quantify the interfacial bonding mechanisms involved at the nanoscale.

It is observed in biological materials such as spider silk that they feature weak bonds (H-bonds) as the primary interactions to define their secondary structure at the molecular scale. Even though the fundamental bonding characteristic is weak, and consists of very small (nanoscale) building blocks, these natural materials still exhibit superior strength, toughness and deformability at the macroscale (for references specific to silk, see e.g. Keten and Buehler, 2008; Buehler, 2010; Keten et al., 2010). In silk, for example, these superior properties are achieved through the grouping of H-bonds in small clusters, which facilitates cooperative deformation (Keten and Buehler, 2008; Buehler, 2010; Keten et al., 2010). Inspired by the mechanical properties of silk and silk-like materials our aim in this paper is to understand and quantify the cooperative deformation of H-bonds in functionalized CNTs in order to provide design guidelines for synthesis and experimental characterization. Specifically, the analysis of H-bond deformation fields is used to compute the extent of significant deformation of bonds that defines the region of cooperativity. The cooperative deformation region in functionalized CNTs is identified by fitting an exponential function to the H-bond deformation, and measuring the associated rate of decay of the deformation denotes the cooperative region. This quantity is then used as a measure for the utilization of the chemical bonds facilitated by the functional groups.

2. Materials and methods

We introduce a simple elastic structural model for CNTs functionalized with carboxyl groups, and study the interaction between CNTs from the perspective of H-bonds formed between the carboxyl groups on each CNT surface. In this mesoscale model, each CNT is modeled as a truss with its stiffness corresponding to the diameter of the CNT. The two H-bonds (from the carboxyl group) that connects the CNTs is also modeled a truss element, where the stiffness of the truss corresponds to two H-bonds. The deformations of H-bonds are studied under an applied shear force. The elastic model introduced here is first used to study the cooperative deformation of H-bonds by grouping the carboxyl groups in pairs of two, three and four on two CNTs. We also study the effect of grouping of CNTs with different diameters.

In our model we assume that the COOH groups are spaced along the sidewalls of the CNTs, but experiments have shown that COOH groups could cluster around the end caps of CNTs (Hirsch and Vostrowsky, 2005; Chiang and Lee, 2009). We systematically include

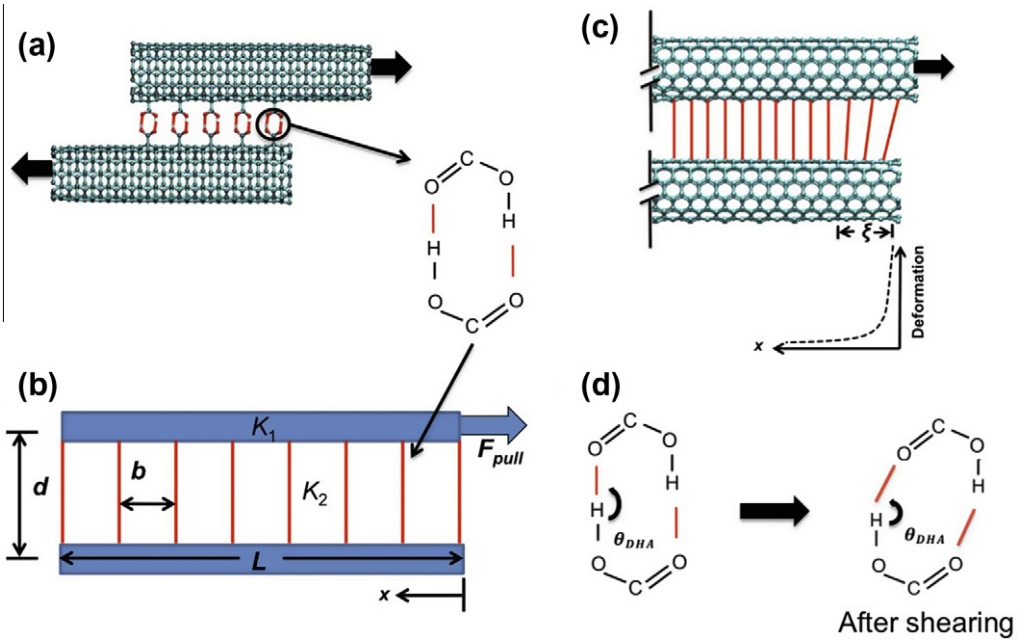

Fig. 1. Geometry of the model considered here. (a) Carbon nanotube functionalized with carboxyl groups under shear loading. (b) A one-dimensional elastic structural model of functionalized CNT, where CNTs are modeled as sheets of stiffness K_1 and are connected by H-bonds of stiffness K_2 between them. The CNTs are at a distance d and of length L. The H-bonds realized by the functional groups are separated by a distance b and the structure is subject to an applied load, here denoted by F_{pull}. Each red line corresponds to two H-bonds as shown in the chemical structure. (c) Deformation of carboxyl groups (red lines) near the end of CNTs under shear loading. The deformation profile shows an exponential decay of displacements along x and the characteristic length ξ is also shown. (d) The carboxyl group before deformation has an initial angle $\angle OHO$ ($\theta_{DHA} = 180^\circ$ initially). After application of shear force the H-bond (OH) undergoes shear deformation. (For interpretation of the references to color in this figure legend, the reader is referred to the web version of this article.)

the clustering of COOH groups near the CNT end caps by considering the non-homogeneous distribution of the COOH groups in our study. In Section 2, we provide an overview of the model and calculation method. In the first subsection we introduce the geometry of the elastic structural model, in the second subsection we describe how we calculate the deformation field as well as the characteristic length, and include the details of the computational procedure utilized to obtain the stiffness parameters of the functional groups and CNTs from the interatomic potential.

2.1. Elastic structural model for carbon nanotube functionalized with carboxyl group

We introduce an elastic structural model to study H-bond deformation in CNTs functionalized with carboxyl groups. In this geometry, the CNTs are connected via H-bonds formed between oxygen and hydrogen atoms of carboxyl (COOH) groups on adjacent CNTs, which are distributed on the surface of CNTs as shown in Fig. 1(a). The elastic structure model is set up accordingly and as shown in Fig. 1(b). Each red line in Fig. 1(b) corresponds to the interaction between two COOH groups connected via two H-bonds. The spacing between the functional groups is b and the CNTs are separated at a distance of d from each other. We use harmonic springs to describe the tension and compression properties of the CNT segment (blue blocks of the length of b in Fig. 1(b)) between any two of the neighboring COOH groups. The stiffness of the CNT segment is $K_1 = K_g/b$, where $K_g = 289$ N/m is the average stiffness of graphene sheet with unit width and unit length (based on atomistic-level modeling reported in (Cranford and Buehler, 2011)) and $w = \pi D$ is the cross-section perimeter of the CNT ($D$is the diameter of CNT). Another set of harmonic springs is applied to describe the two COOH groups connected via a pair of H-bonds (red lines of the length of d in Fig. 1(b)). The shearing stiffness of these springs is K_2 and is a function of the hydrogen bond energy (see Section 2.3). We use a simple model of two basic elements to investigate the tensile property of this CNT junction because it is found to be valid and efficient for studying the deformation along the low dimensional systems (Qin and Buehler, 2010).

We stretch one end of each CNT to investigate the force–deformation relationship of the CNT junction as shown in Fig. 1. The displacement X_j for each atom connecting to a carboxyl group j, under stretching can be solved through the system of equations:

$$K_{ij}X_j = F_i \tag{1}$$

where K_{ij} denotes the component (i,j) of the stiffness matrix and F_j is the external applied force at each carboxyl group. The subscript i and j are Einstein notations for the index of each carboxyl group. We pull the top CNT with a force $F_1 = F_{pull}$, the bottom CNT with a force $F_{2n} = -F_{pull}$ as shown in Fig. 1(a) and (c) and $F_i = 0$ ($i \neq 1, 2n$), where n represents the number of carboxyl groups on each CNT. The K_{ij} matrix is build by assembling the stiffness of each carboxyl group. A detailed description and complete derivation of this approach is given in an earlier paper (Qin and Buehler, 2010).

2.2. Computation of deformation field and characteristic length

We obtain the deformation of each carboxyl group via the elastic model described above and (as described in Section 3) observe that the carboxyl group nearest to the applied force has the maximum deformation, where the deformation decays quickly as the node is located further away from the loading point. This is because the CNT "backbone" is not rigid, and thus the deformation is not uniform but decreases in the direction opposite to the applied force. This phenomenon of decaying displacements can be effectively described by an exponential decay equation (Buehler, 2008) $d\Delta x/dx \sim -\Delta x$ since the elastic deformation of the CNT "backbone" depends on the applied force. Such a relationship is widely used to study how one quantity decreases with respect to an increasing scalar. By solving this equation we obtain

$$x = Ae^{(-x/\xi)} \tag{2}$$

where A is the deformation of the first carboxyl group close to the force point proportional to the applied force F_{pull}, x is the coordinate of the bond as defined in Fig. 1(b), and ξ denotes the rate of decay of the exponential function which is independent of the level of the applied force, F_{pull} (Qin and Buehler, 2010). Following this approach we define a characteristic length scale, ξ, from the fits of displacements to the exponential function defined in Eq. (2). For our specific case this defines a characteristic length scale associated with the number of carboxyl groups that deform more significantly, and therefore the length is adopted to define the size of the cooperative deformation of carboxyl groups, and, more fundamentally, the H-bonds. We therefore use Eq. (2) to fit the deformation of carboxyl groups and use ξ to identify the size of the cooperative deformation of functionalized CNTs under shear loading, where a larger value of ξ means more carboxyl groups in the vicinity of the force application point deform uniformly (see Fig. 1(c)).

2.3. Stiffness of H-bonds

In this section we explain how the parameter K_2, the shearing stiffness of carboxyl groups, is obtained from the interatomic potential. We first calculate the bond energy of each single H-bond to reach the stiffness of each carboxyl group (of two H-bonds). The calculation is based on the Dreiding force field model (Mayo et al., 1990), in which the H-bond energy is given by

$$E_{hb} = D_{hb}\left[5\left(\frac{R_{hb}}{R_{DA}}\right)^{12} - 6\left(\frac{R_{hb}}{R_{DA}}\right)^{10}\right]\cos^4(\theta_{DHA}), \tag{3}$$

where $D_{hb} = 9.5$ kcal/mol has the physical meaning as the depth of the H-bond energy and $R_{hb} = 2.75$ Å as the zero force distance for the H-bond if $\cos(\theta_{DHA})$ keeps constant, and those two are parameters from Dreiding model for the H-bond. The parameter R_{DA} is the distance between the donor (O covalently connect to H here) and the acceptor (O not covalently connect to H here), and (θ_{DHA}) is the angle for $\angle OHO$ as shown in Fig. 1(d). The reason to choose the Dreiding force field to describe the force-extension behavior of hydrogen bonds is that it provides an explicit expression of the hydrogen bond energy as a function of the bond length and the bond angular. Other force fields (e. g. CHARMM, AMBER, etc.) that consider the hydrogen bonding energy implicitly by the combination of vdW and electrostatic interactions make the theoretical deviation too complex and lack of physical meaning. By using this expression, we obtain an explicit expression of the elastic stiffness of the H-bond. Since the length of the covalent bond O–H is $a_1 = 0.98$ Å in the Dreiding force field, by taking the average distance between two neighboring carboxyl groups as a constant, the geometric variants in Eq. (3) can be expressed as (Qin and Buehler, 2010):

$$R_{DA} = \sqrt{x^2 + R_{hb}}, \quad \text{and} \tag{4}$$

$$\cos(\theta_{DHA}) = -\frac{R_{hb} - a_1}{\sqrt{(x^2 + (R_{hb} - a_1))^2}} \tag{5}$$

where x is the shearing displacement of the donor relative to the acceptor. The related atomic parameter values are obtained from the Dreiding force field (Mayo et al., 1990).

With numerical values of all parameters determined, we can now solve the reaction force for all H-bonds within a carboxyl group under shearing as:

$$F = \frac{\partial(mE_{hb})}{\partial x} = D_{hb}\left[60\left(-\frac{R_{hb}^{12}}{R_{DA}^{13}}+\frac{R_{hb}^{10}}{R_{DA}^{11}}\right)\frac{dR_{DA}}{dx}\cos^4(\theta_{DHA}) - \left(5\frac{R_{hb}^{12}}{R_{DA}^{13}}+6\frac{R_{hb}^{10}}{R_{DA}^{11}}\right)4x(R_{hb}-a_1)^2\right]^3, \quad (6)$$

where $m = 2$ is the number of hydrogen bonds within a carboxyl group and the elastic stiffness of carboxyl groups bonded at each node under deformation as:

$$K_2 = \frac{N\partial F}{\partial x}\Big|_{x=0} = \frac{4NmD_{hb}}{(R_{hb}-a_1)^2} \quad (7)$$

where N is the number of carboxyl groups that are grouped together for each node. It is noted that here we take an assumption that stiffness of the carboxyl group are as the function of the hydrogen bond stiffness because the C–C bond energy is an order of magnitude larger than a weak H-bond. We derive the linear elastic modulus of a single carboxyl group as 1686 pN/Å, which is based on its response upon shear loading around the equilibrium state. Without this assumption, it is true that the tangent modulus is nonlinear with its elongation in the x-direction.

3. Results and discussion

We investigate the deformation field of carboxyl groups in functionalized CNTs under shear deformation, following the loading condition depicted in Fig. 1(b). We study two CNTs that are functionalized with carboxyl groups to determine the optimum characteristic length for different groupings of carboxyl groups.

The cooperativity of carboxyl groups is found by plotting the H-bond deformation profile of carboxyl groups attached to CNTs under various levels of grouping. The carboxyl groups are grouped as $N = 1$, 2, 3 and 4, where $N = 1$ corresponds to no grouping, $N = 2$ corresponds to group of two and so on (see Fig. 2(a)). The carboxyl groups are placed at a distance of $b = 8.526$ Å on CNTs of length $L = 200$ Å for the no grouping case and for the groupings of $N = 2$, $b = 17.83$ Å, $N = 3$, $b = 28.014$ Å and for $N = 4$, $b = 39.22$ Å such that the total number of carboxyl groups per unit length remains constant. We begin our analysis for a CNT of diameter $D = 3.2$ Å (this diameter corresponds to $w = 10$ Å and $K_1 = 33{,}890$ pN/Å in our elastic model). This diameter corresponds to the smallest CNT that can be manufactured (Zhao et al., 2004) and is used here as a reference value to start the analysis.

We plot the deformation profile of carboxyl groups for $N = 1$, 2, 3 and 4 and we observe that the carboxyl group deformation is non-uniform (Fig. 2(b)) with the maximum deformation near the applied force, whereas it drops to smaller values for the inner bonds. In order to allow for a direct comparison of the drop in normalized deformation as x increases for each grouping case, the distance x is normalized by $b = 8.526$ Å for the no grouping case ($N = 1$), for $N = 2$, $b = 17.83$ Å, for $N = 3$, $b = 28.014$ Å and for $N = 4$, $b = 39.22$ Å,

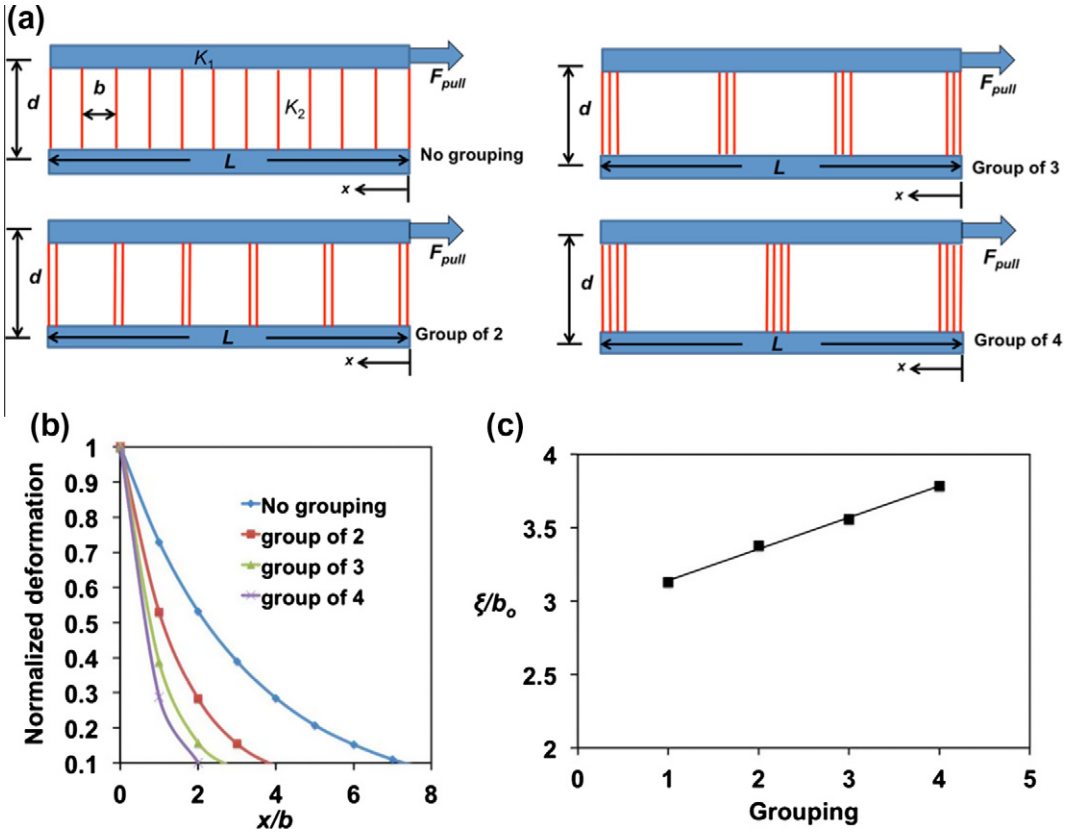

Fig. 2. (a) Variation of geometry, where the grouping is changed from no grouping to groups of $N = 2$, 3 and 4. Each carboxyl group comprises of a pair of two H-bonds; indicated as a red line in the figure. For a length of $L = 200$ Å the carboxyl groups are spaced at $b = 8.526$ Å for the no grouping case ($N = 1$), for $N = 2$, $b = 17.83$ Å, for $N = 3$, $b = 28.014$ Å and for $N = 4$, $b = 39.22$ Å, respectively. The total number of carboxyl groups per unit length is constant. (b) Comparison of normalized deformation of H-bonds for different cases of carboxyl groups shows how deformation drops as the grouping increases. Here the distance x is normalized by $b = 8.526$ Å for the no grouping case ($N = 1$), for $N = 2$, $b = 17.83$ Å, for $N = 3$, $b = 28.014$ Å and for $N = 4$, $b = 39.22$ Å, respectively. (c), Variation of the normalized characteristic length (ξ/b_0) as N is increased shows that the normalized characteristic length increases as the grouping increases, where $b_0 = 8.526$ Å (the distance b for $N = 1$ case). The value of ξ increases as the grouping is increased, from ≈27 Å to approximately 39.22 Å for the case of $N = 4$, marking a 44% increase. (For interpretation of the references to colour in this figure legend, the reader is referred to the web version of this article)

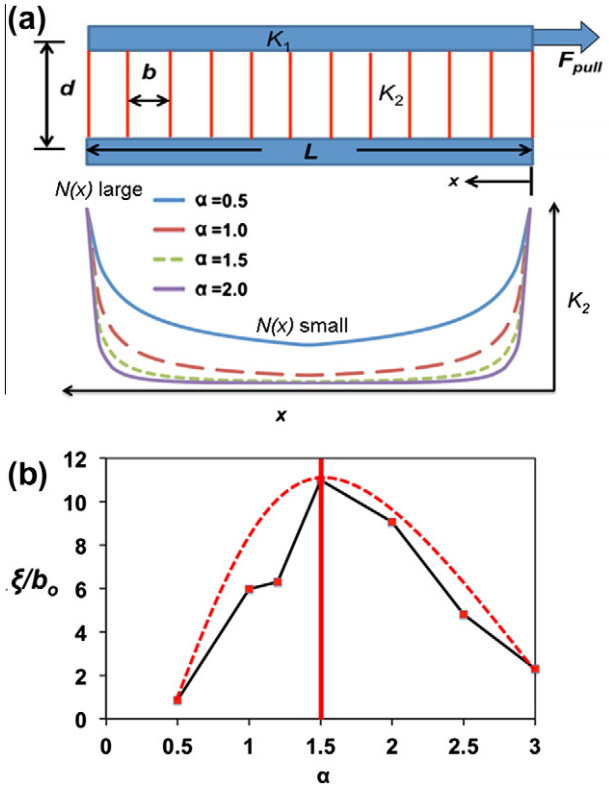

Fig. 3. (a) The variation of stiffness K_2 along the length for different alpha values for a CNT of diameter $D = 3.2$ Å. (b) Cooperative length as a function of non-uniform distribution of the clustering of carboxyl groups, achieved by making $N = N(x)$. The results show that corresponding to $\alpha = 1.5$ yields a maximum cooperative length as 93.76 Å, significantly increased from ≈27 Å for the case of no grouping and uniform distribution (Fig. 2).

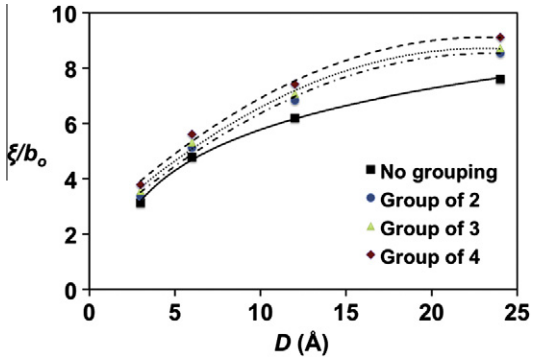

Fig. 4. Variation of characteristic length for no grouping and groupings of $N = 2$, 3 and 4 as a function of CNT diameter D shows that as the CNT diameter increases, the normalized characteristic length increases. As the grouping increases the normalized characteristic length also increases. This result is important since it reveals that the effect of structural organization of functional groups is not only seen in very small diameter CNTs, but that larger diameter CNTs also benefit from the effect of grouping functional groups.

respectively. It is observed that as the grouping of carboxyl groups increases from no grouping to $N = 2$, 3 and 4, the maximum deformation of carboxyl groups drops, with the inner bonds deforming more uniformly as shown in Fig. 2(b). The rate of drop in deformation from the maximum deformation of carboxyl groups is studied by fitting an exponential curve (Eq. (2)) to the carboxyl group deformation. By fitting the deformation profile to an exponential function for a CNT with diameter $D = 3.2$ Å and $N = 1$, the normalized characteristic length ξ/b_0 is obtained as 3.13, where $b_0 = 8.526$ Å (the distance b for the $N = 1$ case). The characteristic length is thus determined as $\xi \approx 27$ Å (see Fig. 2(c)). The characteristic length provides a measure for the "ideal" overlap length between the CNTs, and when the length L is greater than this characteristic length there is limited cooperative deformation among the carboxyl groups. Similarly, the characteristic length is computed for $N = 2$, 3 and 4 cases and it is observed that, as the grouping of carboxyl groups increases the normalized characteristic length increases, as shown in Fig. 2(c). The absolute value of the characteristic length ξ increases as the grouping is increased, from ≈27 Å to ≈39 Å for the case of $N = 4$, marking a 44% increase.

We next investigate whether by varying the distribution of the density carboxyl groups along the CNT axis, the characteristic length ξ can be increased. The deformation of each carboxyl group, as a function of x, is given by the function $\Delta x(x)$. The tensile force thereby can be obtained as $F(x) = -(d\Delta x/dx)bK_1$. Since $dF(x)/dx = -\Delta x K_2/b$, we have $d^2\Delta x/dx^2 = \Delta x K_2/(b^2K_1)$. Thereby the displacement is given by $\Delta x = A_1 \exp(x\sqrt{K_2/K_1}/b) + A_2 \exp(-x\sqrt{K_2/K_1}/b)$ where A_1 and A_2 are constants. Since for $x \to \infty$, $\Delta x \to 0$, we have $\Delta x = A_2 \exp\left(x\sqrt{K_2/K_1}/b\right)$, which yields the deformation profile shown in Fig. 2(b).

The analysis suggests there are two approaches to increase the characteristic length ξ: (i): We can choose $K_1 \to \infty$ (i.e. increase the stiffness of CNTs), which leads to $-x\sqrt{K_2/K_1}/b \to 0$ and thereby $\Delta x = A_2$ approaches a constant value. However, it is difficult to achieve this because for carbon nanotubes, the stiffness of CNTs is controlled by its diameter. (ii) We can adjust the grouping and change the grouping along the axis of the CNT, making $N = N(x)$ in order to reach a decreasing K_2 as a function of the distance from the loading point. Here we take $K_2(x, x \leqslant L/2) = Ax^{-\alpha}$ (by controlling $N = N_0x^{-\alpha}$ as seen in Eq. (7)), where α is a positive dimensionless factor as shown in Fig. 3(a). It is noted because of the symmetric force condition, the other half is given by $K_2\ (x, x > L/2) = A(L - x)^{\alpha}$. We test different values of α with $K_1 = 33{,}890$ pN/Å and a spacing of $b = 8.526$ Å and observe the cooperative length as a function of α as given by Fig. 3(b). It is shown that $\alpha = 1.5$ corresponds to the maximum cooperative length of 93 Å, which is approximately five times the original characteristic length. While manufacturing such CNTs with distributed densities of carboxyl groups may be difficult, this result points to a possible engineering design that can vastly improve the performance of CNT fibers.

We also extend our study to investigate CNTs of different diameters to compute the characteristic length. A wide range of stiffnesses is introduced in the model by varying the stiffness K_1, reflecting CNTs of different diameters. The variation of the characteristic length for different diameters is shown in Fig. 4. As confirmed in Fig. 4, the normalized characteristic length increases with diameter D and this trend is seen irrespective of the grouping of carboxyl groups. As the grouping increases from $N = 1$ to 4 for a CNT of diameter $D = 24$ Å the normalized characteristic length ξ/b_0 increases by 20%, this increase is independent of the CNT diameter and thus reflects the exclusive effect of grouping of carboxyl groups. This result is important since it reveals that the effect of structural organization of functional groups is seen not only in very small diameter CNTs, but larger diameter CNTs are also sensitive to the nanoscale organization.

4. Conclusion

In this paper we analyzed the size of region in which H-bond deformation in functional groups attached to CNTs is cooperative, focusing specifically on CNTs functionalized with carboxyl groups as a model system. We find that for ultra-small CNTs the external force deforms H-bonds significantly only within a relatively small region on the order of a few nanometers. Grouping of functional

carboxyl groups can be used to control the characteristic length in CNT fibers. We identified the use of grouping, as well as a change of the density of functional groups along the CNT axis, as potential strategies to improve the mechanical performance of CNT fibers. Experiments have shown that carboxyl groups can indeed be grown on the surface of CNTs (Ganguli et al., 2008; Liang et al., 2009). Hence, our predictions could potentially be tested and act as guidelines for the design of novel functionalized CNT fibers.

The key result of the analysis is that the effect of structural organization of functional groups is not only significant in very small diameter CNTs that can be made (those with less than 1 nm diameter). Rather, even larger diameter CNTs, as they are most commonly used for engineering applications, are also sensitive to the nanoscale organization of functional groups. We find that larger diameter CNTs naturally show a larger cooperative deformation range, which provides a good basis for further improvement by adding structured functional groups. As in the case of protein materials such as silk, where the nanoscale organization of H-bonds is critical for the mechanical behavior at larger scales, in the case of functionalized CNTs, this design parameter does play an equally important role. The effective cooperative length in large-diameter CNTs is actually very large (tens and hundreds of nanometers), which is an advantage for engineering applications.

Moving forward, our model could be directly applied to other functional groups attached to CNTs, protein and polymer materials, and aid in the design of novel bio-inspired materials. Applications could in principle also include strong bonds such as covalent or ionic bonds, and focus on other weak bonds such van der Waals forces or dipole–dipole interactions. Stronger bonds like covalent bonds could lead to less cooperative deformation with stress singularity at the end of the interface and weaker bonds could result in more cooperative deformation with no stress singularity at the end of the interface.

Acknowledgements

This material is based up on work supported by the US Army Research Laboratory and the US Army Research Office under Grant No. W911NF-09-1-0541.

References

Amr, I.T., Al-Amer, A., Thomas, S., Al-Harthi, P.M., Girei, S.A., Sougrat, R., Atieh, M.A., 2011. Effect of acid treated carbon nanotubes on mechanical, rheological and thermal properties of polystyrene nanocomposites. Composites Part B-Engineering 42 (6), 1554–1561.

Bratzel, G.H., Cranford, S.W., Espinosa, H., Buehler, M.J., 2010. Bioinspired noncovalently crosslinked "fuzzy" carbon nanotube bundles with superior toughness and strength. Journal of Materials Chemistry 20 (46), 10465–10474.

Buehler, M.J. (Ed.), 2008. Atomistic Modeling of Materials Failure. New York, Springer.

Buehler, M.J., 2010. Tu(r)ning weakness to strength. Nano Today 5 (5), 379–383.

Chen, J., Liu, H.Y., Weimer, W.A., Halls, M.D., Waldeck, D.H., Walker, G.C., 2002. Noncovalent engineering of carbon nanotube surfaces by rigid, functional conjugated polymers. Journal of the American Chemical Society 124 (31), 9034–9035.

Cheng, Q., Wang, B., Zhang, C., Liang, Z., 2010. Functionalized carbon-nanotube sheet/bismaleimide nanocomposites: mechanical and electrical performance beyond carbon-fiber composites. Small 6 (6), 763–767.

Chiang, Y.C., Lee, C.Y., 2009. Changes in material properties and surface fractality of multi-walled carbon nanotubes modified by heat and acid treatments. Journal of Materials Science 44 (11), 2780–2791.

Choudhury, A., Kar, P., 2011. Doping effect of carboxylic acid group functionalized multi-walled carbon nanotube on polyaniline. Composites Part B-Engineering 42 (6), 1641–1647.

Coleman, J.N., Khan, U., Gun'ko, Y.K., 2006. Mechanical reinforcement of polymers using carbon nanotubes. Advanced Materials 18 (6), 689–706.

Cornwell, C.F., Welch, C.R., 2011. Very-high-strength (60-GPa) carbon nanotube fiber design based on molecular dynamics simulations. Journal of Chemical Physics 134 (20), 204708.

Cranford, S., Buehler, M.J., 2011. Twisted and coiled ultralong multilayer graphene ribbons. Modelling and Simulation in Materials Science and Engineering 19 (5).

Dhullipudi, R.B., Dobbins, T.A., Adiddela, S.R., Zheng, Z., Gunasekaran, R.A., Lvov, Y.M., 2005. Noncovalent functionalization of single walled carbon nanotubes using alternate layer-by-layer polyelectrolyte adsorption for nanocomposite fuel cell electrodes. Materials Research Society Symposium Proceedings 837 (27), 109–114.

Fam, D.W.H., Palaniappan, A., Tok, A.I.Y., Liedberg, B., Moochhala, S.M., 2011. A review on technological aspects influencing commercialization of carbon nanotube sensors. Sensors and Actuators B-Chemical 157 (1), 1–7.

Ganguli, S., Roy, A.K., Anderson, D.P., 2008. Improved thermal conductivity for chemically functionalized exfoliated graphite/epoxy composites. Carbon 46 (5), 806–817.

Guo, Z., Mao, J., Ouyang, Q., Zhu, Y.Z., He, L., Lv, X., Liang, L., Ren, D.M., Chen, Y.S., Zheng, J.Y., 2010. Noncovalent functionalization of single-walled carbon nanotube by porphyrin: dispersion of carbon nanotubes in water and formation of self-assembly donor–acceptor nanoensemble. Journal of Dispersion Science and Technology 31 (1), 57–61.

Hirsch, A., Vostrowsky, O. (Eds.), 2005. Functionalization of Carbon Nanotubes. Springer-Verlag, Berlin, Heidelberg.

Iijima, S., 1991. Helical microtubules of graphitic carbon. Nature 354 (6348), 56–58.

Jacobs, C.B., Vickrey, T.L., Venton, B.J., 2011. Functional groups modulate the sensitivity and electron transfer kinetics of neurochemicals at carbon nanotube modified microelectrodes. Analyst 136 (17), 3557–3565.

Keten, S., Buehler, M.J., 2008. Geometric confinement governs the rupture strength of H-bond assemblies at a critical length scale. Nano Letters 8 (2), 743–748.

Keten, S., Xu, Z.P., Ihle, B., Buehler, M.J., 2010. Nanoconfinement controls stiffness, strength and mechanical toughness of beta-sheet crystals in silk. Nature Materials 9 (4), 359–367.

Kong, J., Chapline, M.G., Dai, H.J., 2001. Functionalized carbon nanotubes for molecular hydrogen sensors. Advanced Materials 13 (18), 1384–1386.

Kostarelos, K., Bianco, A., Prato, M., 2009. Promises, facts and challenges for carbon nanotubes in imaging and therapeutics. Nature Nanotechnology 4 (10), 627–633.

Koziol, K., Vilatela, J., Moisala, A., Motta, M., Cunniff, P., Sennett, M., Windle, A., 2007. High-performance carbon nanotube fiber. Science 318 (5858), 1892–1895.

Liang, Q., Wang, W., Moon, K.-S., Wong, C.P., 2009, Thermal Conductivity of Epoxy/Surface Functionalized Carbon Nano Materials. IEEE 59th Electronic Components and Technology Conference, vols. 1–4, pp. 460–464.

Mayo, S.L., Olafson, B.D., Goddard, W.A., 1990. Dreiding – a generic force-field for molecular simulations. Journal of Physical Chemistry 94 (26), 8897–8909.

Ostojic, G.N., Ireland, J.R., Hersam, M.C., 2008. Noncovalent functionalization of DNA-wrapped single-walled carbon nanotubes with platinum-based DNA cross-linkers. Langmuir 24 (17), 9784–9789.

Peng, H., Jain, M., Li, Q., Peterson, D.E., Zhu, Y., Jia, Q., 2008. Vertically aligned pearl-like carbon nanotube arrays for fiber spinning. Journal of the American Chemical Society 130 (4), 1130–1131.

Prato, M., Campidelli, S., Klumpp, C., Bianco, A., Guldi, D.M., 2006. Functionalization of CNT: synthesis and applications in photovoltaics and biology. Journal of Physical Organic Chemistry 19 (8–9), 531–539.

Pugno, N.M., 2006. On the strength of the carbon nanotube-based space elevator cable: from nanomechanics to megamechanics. Journal of Physics-Condensed Matter 18 (33), S1971–S1990.

Qin, Z., Buehler, M.J., 2010. Cooperative deformation of hydrogen bonds in beta-strands and beta-sheet nanocrystals. Physical Review E 82 (6).

Su, B., Tang, D., Tang, J., Li, Q., Chen, G., 2011. An organic–inorganic hybrid nanostructure-functionalized electrode for electrochemical immunoassay of biomarker by using magnetic bionanolabels. Analytical Biochemistry 417 (1), 89–96.

Tang, D.P., Su, B.L., Tang, J., Li, Q.F., Chen, G.N., 2011. An organic–inorganic hybrid nanostructure-functionalized electrode for electrochemical immunoassay of biomarker by using magnetic bionanolabels. Analytical Biochemistry 417 (1), 89–96.

Zhao, X., Liu, Y., Inoue, S., Suzuki, T., Jones, R.O., Ando, Y., 2004. Smallest carbon nanotube is 3 angstrom in diameter. Physical Review Letters 92 (12).

Zhu, Z., Song, W., Burugapalli, K., Moussy, F., Li, Y.L., Zhong, X.H., 2010. Nano-yarn carbon nanotube fiber based enzymatic glucose biosensor. Nanotechnology 21 (16), 165501.